Journal of
Marine Science and Engineering

MDPI

Article

Multi-Attribute Decision-Making Ship Structural Design

Tiago Pereira and Yordan Garbatov *

Centre for Marine Technology and Ocean Engineering (CENTEC), Instituto Superior Técnico, Universidade de Lisboa, 1049-001 Lisbon, Portugal; tiagobp@live.com.pt
* Correspondence: yordan.garbatov@tecnico.ulisboa.pt

Abstract: This study develops a procedure for performing multi-attribute decision-making ship structural design of a multi-purpose ship. The already designed ship is further structurally designed to comply with the requirements of the Classification Societies. The ship hull and structural components are verified against yielding, buckling, and ultimate strength. Based on the ultimate limit state (ULS), the first order reliability method (FORM) is employed to analyse the structural risk in reducing the probability of failure. The costs associated with materials, manufacturing, and labour are estimated. The structural risk analysis is performed, accounting for different hazard issues related to loss of ship, loss of cargo, loss of human life, and accidental spill of fuel and oil. The risk-based analysis is used to identify an optimum level of ship structural safety, i.e., the optimum reliability index, controlling the risk associated with the ship hull design. The study uses a multiple attribute decision-making ship design approach, simultaneously considering several objectives for different scenarios employing the Technique of Order Preference by Similarity to Ideal Solution (TOPSIS). The identified ship design solution is associated with the minimum expected total cost leading to lower construction and operational costs and risk with maximum cargo capacity and energy efficiency. The developed procedure is flexible enough to accommodate different design criteria and possible hazards during the ship's service life.

Keywords: ship; design; reliability; failure; capital expenditure; operation expenditure; energy efficiency

Citation: Pereira, T.; Garbatov, Y. Multi-Attribute Decision-Making Ship Structural Design. *J. Mar. Sci. Eng.* **2022**, *10*, 1046. https://doi.org/10.3390/jmse10081046

Academic Editor: Decheng Wan

Received: 19 June 2022
Accepted: 25 July 2022
Published: 29 July 2022

1. Introduction

The ship structural design consists of an iterative decision-making process involving various aspects, such as the type of service, cargo transported, velocity, etc., to determine the optimal ship and structural configuration. One of the objectives of ship design is to identify an efficient and environmentally friendly design solution.

The International Maritime Organization (IMO) developed rules and guidelines that regulated the ship's design to maintain safety in the maritime sector. In 1969, IMO gave responsibility for applying maritime safety rules and standards to the International Association of Classification Societies (IACS). Due to increased competition in the maritime sector, which already accounts for about 90% of world trade, it is necessary to design and optimise more efficient ships with a reasonable safety level for a lower construction, operation, and dismantling expenditure and not only to comply with the minimum requirements, as defined by IACS, but to create safety and environmentally friendly ships.

The ship design goes through a series of evolutionary stages converging to a single design solution, where the most traditional method is the spiral design [1]. Different optimisation techniques have been employed to solve the ship design problem, traditionally being a sequential and iterative process, allowing for developing more competitive design solutions. Nowacki, et al. [2] developed computer-aided design and optimisation algorithms, and Hughes [3] and Hughes, et al. [4] established the essential steps in optimising the ship structures.

Optimisation tools are currently taking a more general approach and becoming more reliable in contrast to what was done in the past, where the optimisation was directed to a

single objective, becoming a limiting factor. To solve these limitations, several studies [5–9] developed design and optimisation techniques, which were later [10,11] incorporated into multi-criteria optimisation models that include the structural weight and cost of production.

IMO adopted risk-based assessment procedures for ship design by defining the formal safety assessment (FSA) [12–15] as a method to enhance maritime safety, protecting human life in the sea, maritime environment, and cargo and ship integrity by employing cost-benefit assessments. Concerns are raised because many already built ships cannot adequately meet the new requirements introduced by IMO, which impacted the risk-based design performance [16] and short sea shipping [17].

Many studies have been performed using the holistic ship design approach in [16,18,19]. A design risk-based framework covering the ultimate limit state and hazards from accidental spills, cargo loss, ship, and crew members was introduced in [18].

A risk-based framework has been developed in a series of studies [19] for ship and structural design and maintenance planning, where the risk analysed covered the structural failure. For structural failure, the time profiles of performance incorporating the structural degradation for structural integrity assessment were also part of the framework [20].

Several aspects related to the ship's structural critical failure modes, type of cargo to which the structure will be subjected during its operational life, and weight and centre of gravity when developing the structural configuration need to be considered when creating a mathematical model that represents the structure, validates the design criteria for different types of failure modes that may occur, and modifies the structural configuration for proper performance and optimisation levels, thus avoiding unnecessary costs. The modern ship designer considers various solutions across performance metrics using the multiple criteria decision-making (MCDM) approach, which involves the selection of the best alternative from pre-specified alternatives [21–23]. The multiple objective decision-making (MODM) alternatives can be set with multiple equality and inequality constraints in the decision space [24,25].

Recently, several studies [26] analysed the operational characteristics of several ship-type design solutions. The studies focused on the main dimensions of ships, intact stability, and seakeeping performance. Particular attention was paid to the vertical bow acceleration, deck wetness, hydrodynamic impact, propeller emersion, motion sickness, and wave-induced water resistance, which leads to additional brake horsepower.

The present study develops a procedure for performing a multi-attribute decision-making multi-purpose ship design. Ship hull design magnification factors (SHDMF)are introduced to generate alternative ship design solutions for an already designed ship. The introduced ship design magnification factors reflect the ship hull structural capacity but also associated risk related to the loss of ship, cargo, human life in the open sea, sea pollution due to accidental fuel and oil spill, construction and operating cost, energy efficiency, and cargo capacity of the ship. Employing MADM, several alternative design solutions are evaluated.

2. Ship Design

Ship design assesses the owner's specification requirements (ship type, dead weight, speed, data of a similar ship, etc.), life cycle cost, and shipyard capabilities. Specification requirements consider ship hull descriptors, shaft horsepower, lightship weight, dead weight, cargo capacity, free board, stability, seakeeping, midship section design, and ultimate strength assessment of ship hull subjected to still water and wave-induced loads, as well as the progressive structural failure. Due to the substantial number of items that need to be considered, the Pareto optimisation algorithm [27,28] is employed to conclude the best design choice in defining the design parameters.

The work presented in [29] analysed the prerequisites for the environmental pollution driven by maritime transportations in adopting a new ship design concept. The new developed risk-based ship design minimises the risk related to environmental pollution while considering the life cycle assessment and energy efficiency of the ship propulsion system. The optimal design solution for the main dimensions and operation characteristics

of a fleet of multi-purpose ships was based on the energy efficiency design index accounting for shipbuilding, operation cost, and resale costs at the end of the service life, where the acceptable design solution involved the requirements for ship resistance, propulsion and stability, free-board, seakeeping, and manoeuvrability.

In the present study, one of the multi-purpose ships that was a part of the fleet designed and analysed in [29] is further developed, concerning the midship section scantling satisfying the additional service grab loading [30] accounting for the structural risk and operational characteristics using MADM [31]. The main dimensions of the ship used for the analysis here are given in Table 1. The main dimensions of the initially designed ship will be kept constant during the study. The ship design solution will be evaluated by introducing ship hull design modification factors.

Table 1. Main Dimensions of Multi-Purpose Ship.

Main Particulars	Value	Units
Rule Length, L	115.07	[m]
Moulded Breadth, B	20.00	[m]
Depth, D	10.40	[m]
Moulded Draught, T	8.30	[m]
Block Coefficient, C_B	0.72	[-]
Maximum Service Speed, V_s	14.00	[knots]
Deadweight, DWT	9800	[tonnes]
Effective Propulsive Power, P_w	5400	[kW]
Number of Crew Members, NE	20	[Pax]
Number of Superstructure Decks, NJ	6	[-]

SHDMFs are employed as a risk control option to allow the design to be modified realistically and identify the effect on the ultimate capacity of the ship hull structure for estimating the reliability beta index, life cycle cost assessment, and resulting risk.

3. Midship Structural Design

The midship section of the multi-purpose ship is designed according to the rules of the Classification Society [30], following the ship structural design principle, loads, motions and accelerations, internal and external pressures, and forces needed for the process of the ship hull structural scantling satisfying the yielding, buckling, and ultimate strength requirements.

The width of plates and the spacing of ordinary stiffeners and girder span is defined, considering that the longitudinal span is two to three times the frame spacing. Normal strength steel is used for building the bottom and close to the neutral axis structural components. The choice of high-tensile steel for the structural elements distant from the neutral axis, in this case, the deck area and the hatch coaming, is due to the significant stresses in those locations (see Figure 1).

The vertical bending moments imposed on the ship hull include the still water, wave-induced bending moments, and respective shear forces estimated as stipulated in [23]. The load cases used for the structural design are load cases “a” and “b” and load cases “c” and “d”, where load cases “a” and “b” refer to the ship in upright conditions, i.e., at rest or having surge, heave, and pitch motions and load cases “c” and “d” refer to the ship in inclined conditions, i.e., sway, roll, and yaw motions [30].

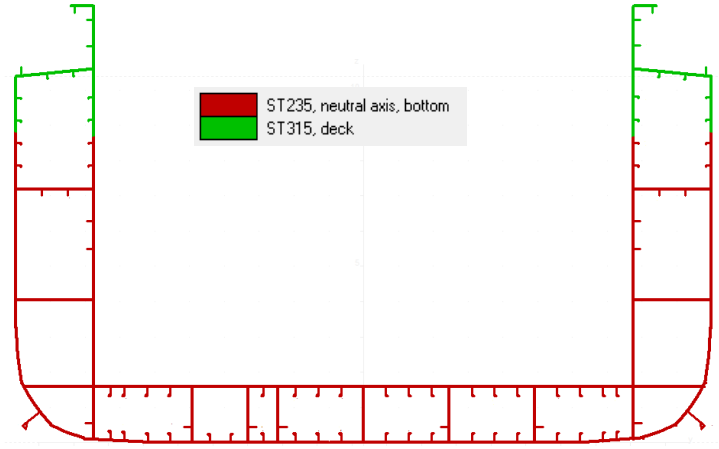

Figure 1. Midship section and material distribution.

The scantling procedure involves decision variables, constraints, and objective functions according to [30]. The decision variables involved in the optimisation process include the ship hull plate thickness, $t_{c,i}$, defined as:

$$t_{min} \leq t_{i,c} \leq t_{max} \tag{1}$$

the material yield stress, σ_y, as a discrete variable, according to the existing shipbuilding steels:

$$\sigma_{y,\,min} \leq \sigma_{y,\,upper\ shell} \leq \sigma_{y,\,max} \tag{2}$$

$$\sigma_{y,\,min} \leq \sigma_{y,\,lower\ shell} \leq \sigma_{y,\,max} \tag{3}$$

The constraints applied are related to the local strength, represented by the minimum plate thickness:

$$t_{i,c} - t_{i,\,min} \geq 0 \tag{4}$$

the minimum section modulus (longitudinal strength) for the deck and bottom are defined as:

$$Z^{deck} - Z^{deck}_{min} \geq 0 \tag{5}$$

$$Z^{bottom} - Z^{bottom}_{min} \geq 0 \tag{6}$$

and the minimum critical buckling stress is defined as:

$$\eta_i \sigma_{c,i} - \sigma_{a,i} \geq 0 \tag{7}$$

where η_i is the usage factor, $\sigma_{a,i}$ is the acting stress, and $\sigma_{c,i}$ is the critical buckling stress.

The scantling of the midship section defines the net thickness of the plate panel subjected to in-plane normal stresses acting on the shorter side, which needs to be not less than the one as defined in [30] in satisfying the yield criteria:

$$t = 14.9\ C_a\ C_r\ s\ l \sqrt{\gamma_R\ \gamma_m \frac{\gamma_{S2}\ p_S + \gamma_{W2}\ p_W}{\lambda_L\ R_y}} \geq t_{min}, \tag{8}$$

where: p_S is the still water pressure and p_w is the wave-induced pressure, s is the shorter side of plating, and l is the longer side of plating, C_a is the aspect ratio of the plate panel, C_r is the coefficient of curvature R_y is the minimum yield stress, and γ_R, γ_m, γ_{S2}, γ_{W2} are utilisation factors.

The minimum net shear sectional area A_{Sh} and the net section modulus W, for ordinary longitudinal stiffener subjected to lateral pressure, are to be not less as defined in [30]:

$$A_{Sh} = 10\,\gamma_R\,\gamma_m\,\beta_S\,\frac{\gamma_{S2}\,p_s + \gamma_{W2}\,p_W}{R_y}\left(1 - \frac{s}{2l}\right)s\,l \tag{9}$$

$$W = \gamma_R\,\gamma_m\,\beta_b\,\frac{\gamma_{S2}\,p_s + \gamma_{W2}\,p_W}{m\left(R_y - \gamma_R\,\gamma_m\,\sigma_{x1}\right)}\left(1 - \frac{s}{2l}\right)s\,l^2\,10^3 \tag{10}$$

where β_S, β_b, m are factors defined in [32].

The ship's structural elements are also subjected to a compressive load, which may lead to a buckling failure. The type of the load and their combinations employed in the current analysis is axial, bending, and shear loadings. The common causes of plate buckling of ship structural components are due to the high compressive and residual stresses, high shear stresses, combined stresses, lack of flexural rigidity, lack of stiffening, significant initial imperfections, extensive and improper use of high tensile steel, and excessive material wastage due to general and local pitting corrosion [32–36].

The general modes of failure of stiffened panels are identified as the lateral buckling of stiffeners, torsional buckling of stiffeners, flexural buckling of stiffeners, flexural buckling for plate stiffener combination, and buckling of plate panels between stiffeners. The combined critical stress σ_{comb}, for plate panels subjected to compressive axial, bending, and shear loads are defined as [30]:

$$F \;\leq\; 1 \text{ for } \frac{\sigma_{comb}}{F} \leq \frac{R_{eH}}{2\gamma_R\gamma_m} \tag{11}$$

$$F \leq \frac{4\sigma_{comb}}{\frac{R_{eH}}{\gamma_R\gamma_m}}\left(1 - \frac{\sigma_{comb}}{\frac{R_{eH}}{\gamma_R\gamma_m}}\right) \text{ for } \frac{\sigma_{comb}}{F} > \frac{R_{eH}}{2\gamma_R\gamma_m} \tag{12}$$

where F, R_{eH} are defined in [30].

The critical buckling stress, σ_c for compressive axial and bending loads is defined as [30]:

$$\sigma_c = \sigma_E \text{ for } \sigma_E \leq \frac{R_{eH}}{2} \tag{13}$$

$$\sigma_c = R_{eH}\left(1 - \frac{R_{eH}}{4\sigma_E}\right) \text{ for } \sigma_E > \frac{R_{eH}}{2} \tag{14}$$

where σ_E is the Euler buckling stress.

The critical buckling stress of the ordinary stiffeners is estimated as [30]:

$$\frac{\sigma_c}{\gamma_R\gamma_m} \geq |\sigma_b| \tag{15}$$

where σ_b is defined in [30].

Bureau Veritas software MARS 2000 [37] is employed to analyse the ship's structural hull girder's ultimate strength. The software adopted the progressive collapse method [31] to analyse the ultimate strength of the hull girder between two adjacent frames [32]. In this analysis, the midship section is divided into structure elements: stiffener attaching plating element and hard corner element, acting independently in their failure modes.

The incremental–iterative approach obtains the moment-curvature relationship [38]. Each iteration's bending moment acting on the hull girder transverse section increases due to the imposed curvature. Each structural component has an axial strain due to the angle of rotation of the hull girder transverse section about its horizontal neutral axis. In the sagging conditions, the structural elements above the neutral axis are shortened, while those below the neutral axis are lengthened. The location of the neutral axis and the cross-section of the ship are calculated based on the failure mode of each structural element as the external

moment is applied. The tensile structural elements represent a single mode of elastic-plastic failure, while in compression, they present the mode of buckling or yielding.

The pink dashed line in Figure 2 shows the applied bending moment the hull girder needs to support [23]. As seen in Figure 2, the higher ultimate strength occurs in the hogging condition and lower in sagging loading conditions, respectively. The worst possible scenario for structure failure appears in the sagging loading condition.

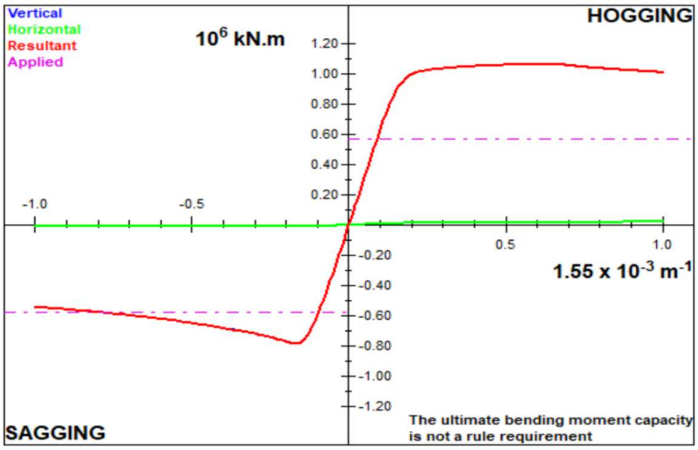

Figure 2. Bending moment-curvature relationship, *SHDMF* = 1, vertical (blue) is the bending moment axis, horizontal (green) is the curvature axis, resultant (red) is the hull girder strength and applied (pink) is the bending moment the hull girder needs to support.

A change in the ultimate strength is most effectively achieved by modifying the thickness of structural components [39,40]. By employing *SHDMF* in the structural analysis, the midship section structure is redesigned, keeping the thickness of the structure closest to the neutral axis constant (inner side and side shell) and changing the thickness of the structure farthest from the neutral axis (bottom, double bottom, and deck structure) where the global failure most probably is expected to occur.

4. Structural Reliability Analysis

The ship hull structural progressive collapse due to the loss of structural stiffness and strength is related to the loss of equilibrium, attainment of the maximum capacity of the resistance by yielding, rupture or fracture and the instability resulting from the buckling or elastoplastic collapse of plating, stiffened panels, and support members, and it is defined as the ultimate limit state. The limit state function in the reliability assessment of the ship hull structure is based on the ultimate strength of the ship hull, as defined in [41]:

$$g(\mathbf{X}) = \widetilde{x}_u \widetilde{M}_u - \left(\widetilde{x}_{sw}\widetilde{M}_{sw} - \widetilde{x}_w \widetilde{x}_s \widetilde{M}_w\right) \tag{16}$$

where $\widetilde{M}_u$ is the ultimate bending moment and $\widetilde{M}_{sw}$ is the still water bending moment fitted to a normal distribution [42]. The regression equations define the statistical descriptors of the still water bending moment as a function of the length of the ship, L and dead-weight ratio, $W = (DWT/\text{Full load})$ [43,44] as:

$$Mean(M_{sw}) = \frac{Mean(M_{sw,max})M_{sw,CS}}{100} \tag{17}$$

$$StDev(M_{sw}) = \frac{StDev(M_{sw,max})M_{sw,CS}}{100} \tag{18}$$

where $M_{sw,CS}$ is the still water bending moment as given in [30] and $Mean(M_{sw,max})$ and $StDev(M_{sw,max})$ are defined as a function of L and W as suggested in [43].

The wave-induced bending moment, $\widetilde{M}_w$ is fitted to the Gumbel distribution [41], $\widetilde{x}_u$ is the uncertainty on ultimate strength, $\widetilde{x}_{sw}$ is the uncertainty prediction on the still water bending moment, $\widetilde{x}_w$ is the uncertainties in the wave-induced bending moment due to linear seakeeping analysis, and $\widetilde{x}_s$ is a factor that accounts for the nonlinearities in sagging load. The uncertainty coefficients $\widetilde{x}_{sw}$, $\widetilde{x}_w$, $\widetilde{x}_s$ are fitted to a normal distribution function, with a mean value of 1.00 and a standard deviation of 0.1. The model uncertainty on ultimate strength $\widetilde{x}_u$ is fitted to a normal distribution function with a mean value of 1.05 and a standard deviation of 0.1. It is assumed that the MARS 2000 software calculates the ultimate bending moment at the confidence level of 5%, where $M_u^{5\%} = M_u^C$ and it is fitted to a log-normal probability density function, where the covariance, *COV*, is 0.08 [45].

The reliability index of the midship hull structure for the net and gross designs is estimated at the end of the service life of the ship, considered here as $\tau_s = 25$ years, assuming that the structure of the ship is entirely corroded, i.e., there is no corrosion margin as determined by the Classification Society rules, concerning the net ship hull structural design, and the gross structural design is considered when the ship structure is not corroded, and the corrosion protection is appropriately functioning. It is also assumed that the structure of the midship section is subjected to general corrosion degradation, where over the years, its degradation has occurred for all structural components. The mean value and standard deviation of the corrosion depth as a function of time is taken as defined in [46], and the statistical descriptors of the vertical wave-induced bending moment are in [41].

Using the first order reliability method [47,48], failure may occur when $g(\mathbf{X})$ fails, leads to $P_f = P(g(\mathbf{X}) < 0)$, which may be evaluated by using the standard normal distribution function as $P_f = P(g(\mathbf{X}) < 0) = \Phi(-\beta)$, where β is the beta reliability index [49].

The time-dependent non-linear beta reliability index, $\beta(t)$, where $t \in [0, \tau_S]$ is defined as [19]:

$$\beta(t) = \beta_{gross} - (\beta_{gross} - \beta_{net})\left(1 - e^{-\frac{t-\tau_c}{\tau_t}}\right),\ t > \tau_c \tag{19}$$

$$\beta(t) = \beta_{gross},\ t < \tau_c \tag{20}$$

where τ_c = 6.50 years is the coating life and τ_t = 11 years is the transition life, β_{gross} is the beta reliability index related to the gross thickness of structural components and β_{net} is related to the net thickness. The time-dependent non-linear Beta reliability index as a function of *SHDMF*s can be seen in Figure 3.

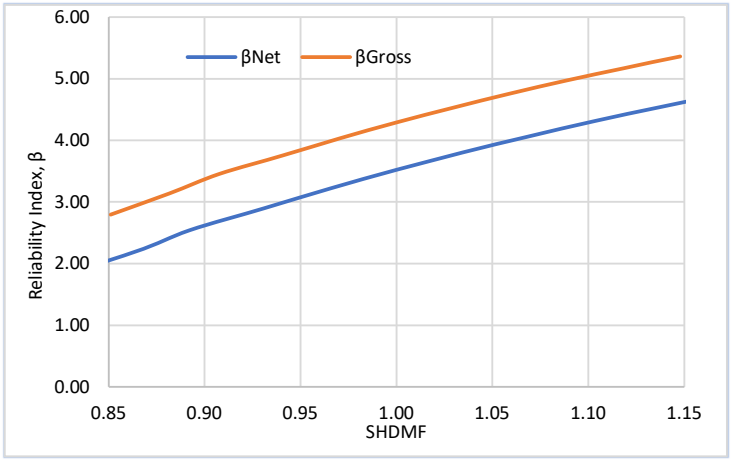

Figure 3. Beta reliability index β for net and gross scantling.

5. Cost–Benefit Analysis

The ship is subjected to corrosion degradation and structural failures during the service life due to progressive structural collapse. To control the risk associated with the

structural collapse of the ship's hull, accounting for the existing uncertainties, based on an identified failure scenario, the risk is measured as a product of the likelihood of structural failure and its consequences defined as:

$$Risk\ (t) = \sum_j P_{f,j}\left(P\left[g\left(X_{1,j}|t\right) \leq 0\right]\right) C_{f,j}\left(X_{2,j}|t\right),\ t\epsilon[0, \tau_s] \tag{21}$$

where $P_{f,j}\left(P\left[g\left(X_{1,j}|t\right) \leq 0\right]\right)$ is the probability of failure, $C_{f,j}(X_2|t)$ is the consequence cost of failure, $X_{1,j}$ and $X_{2,j}$ are the vectors of parameters involved in the probability of failure and consequence analyses that occur during the service life of the ship τ_s.

The objective is to reduce the risk to an acceptable level by optimising the ship's hull structure and evaluating alternative decision-making options. The method used to define the acceptable risk is through the reliability index that minimises the cost of the structure's design, where various failure modes may result in economic, environmental, and human losses and other consequences.

The risk, $Risk(t^n|SHDMF, \beta)$ is defined as [19]:

$$Risk(t^n|SHDMF, \beta) = C_{Pf}\ (t^n|SHDMF, \beta) + C_{me}(SHDMF, \beta) \tag{22}$$

where $C_{Pf}\ (t^n|SHDMF, \beta)$ is the cost associated with the structural failure over the service life of the ship and $C_{me}(SHDMF, \beta)$ is the cost of implementing a structural safety measure accounting for *SHDMF*, including the cost of material and labour needed to redesign the ship hull structure.

The life cycle cost (LCC) of the ship is defined as the total cost of all distinct phases of life of the ship and its equipment, including design, acquisition, operation, maintenance, upgrade, and dismantling. It is defined as a sum of cost estimates from the beginning to the end of the life cycle and is used in the design process of all engineering systems, including ships [20,29,31] and offshore structures. The total costs of the ship related to the distinct phases of the ship's life cycle are divided into three diverse groups, including capital expenditure (CAPEX), operating expenditure (OPEX), and dismantling expenditure (DECEX).

The MARAD [50] system is used for the group-specific ship systems and their associated costs. The systems groups are based on the different components in constructing the ship's life cycle, and their costs are included in the construction project.

The initial capital cost estimate for constructing multi-purpose ships is based on several design parameters, such as main dimensions, dead-weight, lightship weight, propulsive power, etc. A regression analysis makes it possible to estimate CAPEX using a mathematical relationship between the input parameters and the cost of construction [51]. Construction costs are divided into four components: material, labour, overheads, and profits. It is assumed that the steel price is 580 EUR/tonne, and the equipment is 1500 EUR/tonne [52].

The annual operating expenditure is a sum of the salary of crew members, costs related to the stores and supplies, insurance, port expenses, and annual fuel cost. The dismantling cost is evaluated as a function of the lightship weight.

The cost associated with the structural failure over the service life of the ship is estimated as a function of *SHDMF*, reliability index, and time [19]:

$$\begin{aligned} C_{pf}(t|SHDMF\ , \beta) \\ = \textstyle\sum_j^n P_f(t_j|SHDMF, \beta)\ [C_S(t_j|SHDMF, \beta) + C_C + C_d \\ + C_v] e^{-\gamma t_j} \end{aligned} \tag{23}$$

where $P_f\left(t_j|SHDMF, \beta\right)$ is the probability of failure, $C_S\left(t_j|SHDMF, \beta\right)$ is the total cost of the ship in the year $t_j\ \in [0,\tau_s]$, C_C is the cost associated with the loss of the cargo, C_d is the cost associated with the accidental spill, C_v is the cost associated with the loss of human life, and γ = 5% is the assumed value of the discount rate (see Figure 4).

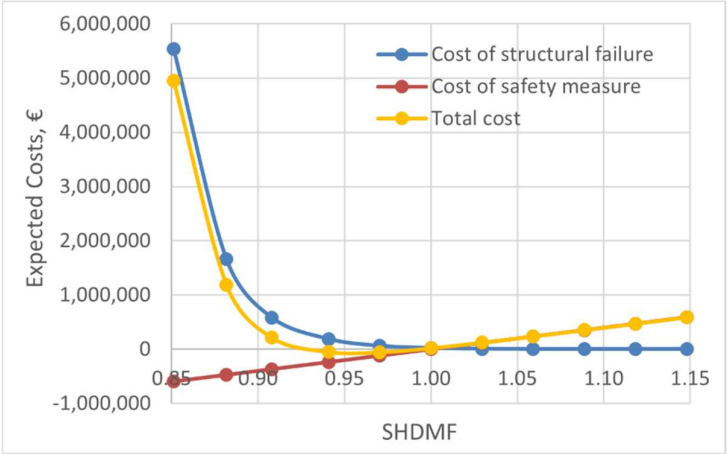

Figure 4. Cost of structural failure, safety measure, and total cost.

The cost of the ship, $C_S(t_j|SHDMF, \beta)$, is a function of the ship's age, that is, the initial cost of the ship, $t_0 = 0$ years, and the scrapping cost $t_n = 25$ years accounting for corrosion degradation [21] is estimated as [46]:

$$\begin{aligned} C_s(t_j|SHDMF, \beta) & \\ &= C_s(t_0|SHDMF, \beta) \\ &-[C_s(t_0|SHDMF, \beta) - C_s(t_n|SHDMF, \beta)][1 - e^{-\frac{t_j - \tau_C}{\tau_t}}],\ t_j \\ &> \tau_C \end{aligned} \tag{24}$$

$$C_s(t_j|SHDMF, \beta) = C_s(t_0|SHDMF, \beta),\ t_j < \tau_C \tag{25}$$

where $C_s(t_0|SHDMF, \beta)$ is the initial cost of the ship, $C_s(t_n|SHDMF, \beta)$ is the scrapping cost, t_j is the year of the operation and C_{scrap} = 270 EUR/tonne is the assumed value of the scrap cost.

The cost associated with the loss of cargo, C_C, is estimated as [39]:

$$C_c = C_{cargo}\ f_{cargo}\ P_{cargo} \tag{26}$$

where C_{cargo} = 1200 EUR/tonne is the assumed cost of a tonne of cargo, f_{cargo} = 20% is the considered partial factor of the cargo lost, and P_{cargo} is the total amount of the cargo of the ship, estimated as 7200 tonnes.

The cost of the accident spill, C_d is estimated as [39]:

$$C_d = f_{spill}\ P_{sl}\ CATS\ W_{fuel\ oil} \tag{27}$$

where f_{spill} = 10% is the considered a partial factor of the fuel oil spill, P_{sl} = 10% is the probability that the fuel oil split reaches the shoreline [36], $CATS$ = 60,000 EUR/tonne [53] is the cost of one tonne of accidentally spilt fuel oil and $W_{fuel\ oil}$ is the total weight of fuel oil in tonnes.

The cost associated with the loss of human life, C_v, related to the loss of crew members is estimated as:

$$C_v = n_{crew} f_{crew}\ ICAF \tag{28}$$

where n_{crew} is the number of crew members, f_{crew} is the probability of loss of the life of a crew member (considered 25%), and $ICAF$ is the implied cost of averting the fatality.

The cost associated with the fatality is based on the implied cost of avoiding a fatality $ICAF$, which uses a risk model obtained from the average of the OCDE countries [54].

The cost of implementing the structural safety measure accounts for the SHDMF, which is also associated with the reliability level, including the cost of material and labour.

The cost of structural safety measures, $C_{me}(SHDMF, \beta)$ is positive or negative depending on if the value of $SHDMF$ is larger or smaller than 1, respectively [39]:

$$C_{me}(SHDMF, \beta) = \Delta W_{steel}(SHDMF, \beta)\, C_{steel} + C_{labour}(SHDMF, \beta) \quad (29)$$

where $\Delta W_{steel}(SHDMF, \beta)$ is the weight of steel, in tonnes, because of the design modifications factor, C_{steel} is the cost of steel, and C_{labour} is the cost of labour. The weight of steel is estimated as [39]:

$$\Delta W_{steel}\ (SHDMF, \beta) = (SHDMF - 1) W_{steel} \quad (30)$$

where W_{steel} is the weight of steel related to the ship hull structural design (see Figure 5).

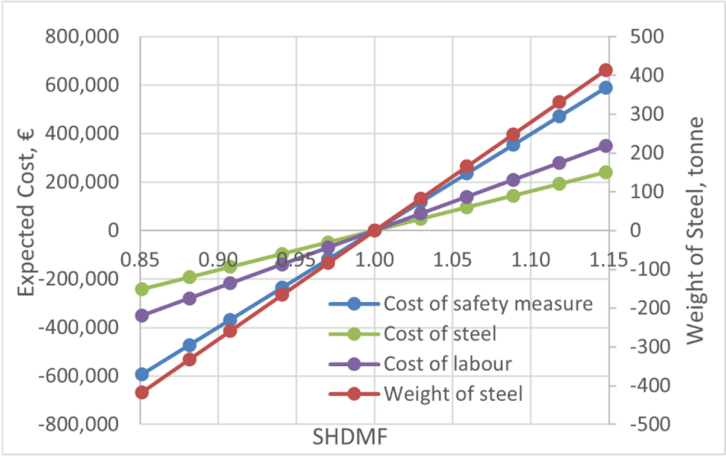

Figure 5. Safety measures, steel and labour cost, and weight of steel.

The cost-benefit analysis is used to identify an optimum level of ship safety, i.e., the optimum reliability index, controlling the risk associated with changing the initial design. The cost-benefit analysis of the redesigned structure, according to the ship hull design magnification factors related to the scantlings of the midship section, is conducted based on the expected total risk.

The target reliability level β reflects the structural failure cost associated with risk control since each cost is a function of the reliability index, see Figure 6. According to the study performed in [55], the range of the target reliability index over the ship's service life can be between 2.79 and 5.38. The most economical target reliability index here is 4.29.

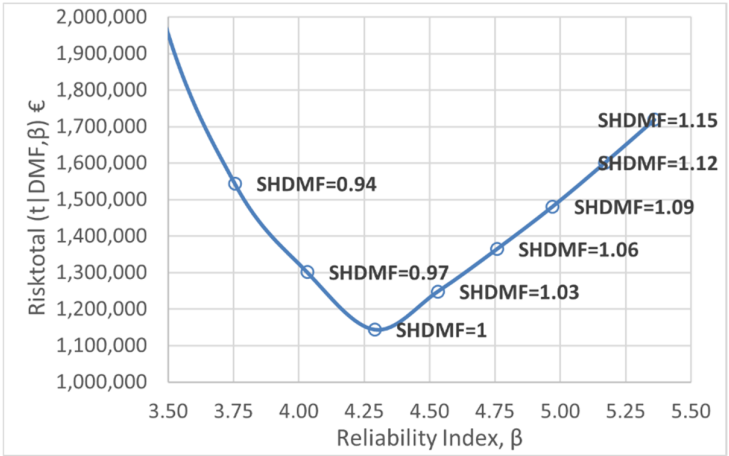

Figure 6. Expected total risk.

There are some difficulties in defining the cost-related parameters, which is explained by the fact that it is necessary to account for factors that impact the cost forecast. This becomes a critical issue due to the long in-service time of ships and the evolution of prices in such an extended period. Time series analysis may be used in economic forecasting. To analyse and forecast prices, an average, naive, random walk or decomposition, exponential smoothing, or autoregressive integrated moving average [56] process may be used.

6. Decision-Making Ship Design

The ship hull structural design is a multiple-objective decision problem, which requires identifying an optimal structural design solution to fulfil the established primary descriptors of the ship and satisfy the constraints. The goal here is to achieve fast and accurate design solutions finalised at minimising the total expected cost and risk, which is a function of numerous factors, including the ship hull strength and cargo capacity, lightship weight, and energy efficiency. Any acceptable design solution needs to follow the ship design criteria related to the free-board, stability, seakeeping, manoeuvrability, etc.

In this regard, additionally to the risk of structural collapse, estimated in monetary terms, it is essential to include in the multiple attribute's decision analysis the annual operating cost, annual construction cost, cargo capacity measured by the number of containers transported, and attained energy efficiency design index as a function of *SHDMF*. The lightship weight is defined as the sum of the weight of the hull structure, equipment, outfitting, and machinery [56,57].

Since the ship weight and buoyancy forces are in balance, any change in the structural design due to the application of the *SHDMF* will reflect the lightship weight *LW*. To keep the predefined draft, trim, and the longitudinal centre of gravity location, the dead weight *DWT* needs to be adjusted in the part of the cargo and ballast content, which will lead to new acting still water bending moment *Msw*. The estimated *LW, DWT* and Msw for the generated design solutions as a function of *SHDMF* are presented in Figure 7.

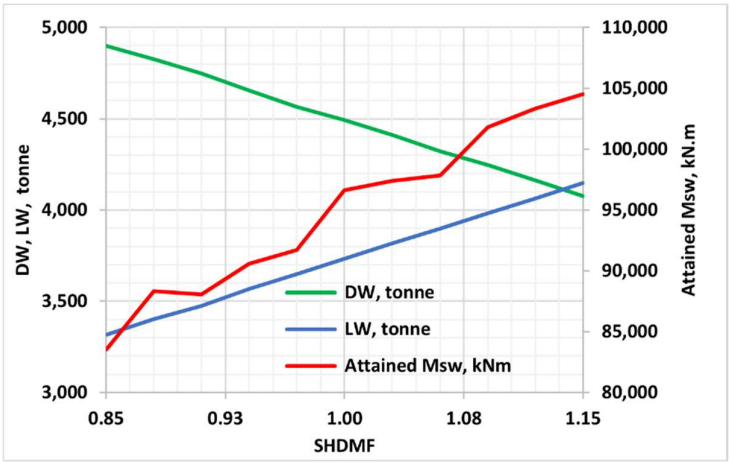

Figure 7. *LW, DW* and steel water vertical bending moment, *Msw* at midship section.

The acting still water bending moments are shown as red circles in Figure 8, and the design still water bending moment, for hogging and sagging, by the green and blue envelopes. As can be seen, the attained still water bending moments as a function of *SHDMF* at the midship section are much below the design one as stipulated in [30]. The difference between the design and acting steel water bending moment will enhance the already established structural reliability index estimated based on the design steel water and wave-induced bending moment and ultimate strength.

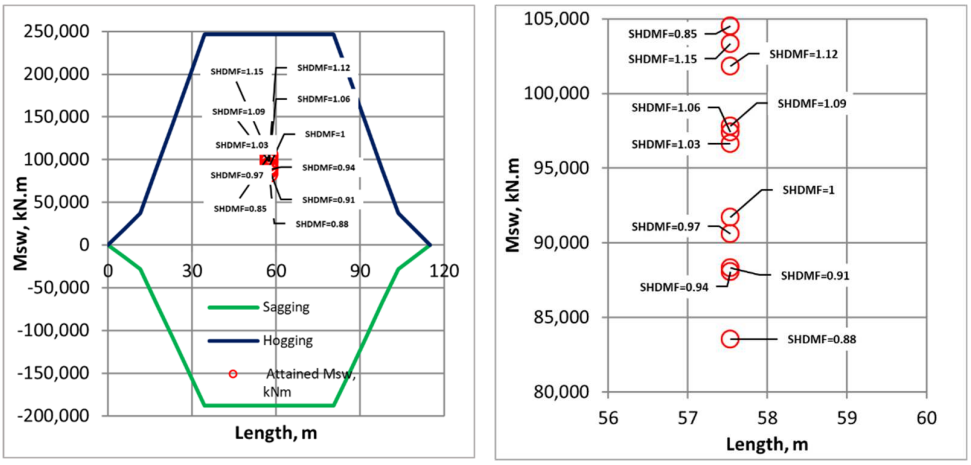

Figure 8. Steel water vertical bending moment at midship section, *Msw*, regular scale (**left**) and magnified scale (**right**).

The operating costs are the ongoing expenses connected with the vessel's day-to-day running (excluding fuel, which is included in voyage costs) and an allowance for everyday repairs and maintenance. Operating costs' principal components include manning costs, stores, routine repair and maintenance, insurance, and administration. The annual operating cost, transported containers, and construction costs, as a function of *SHDMF*, are given in Figure 9.

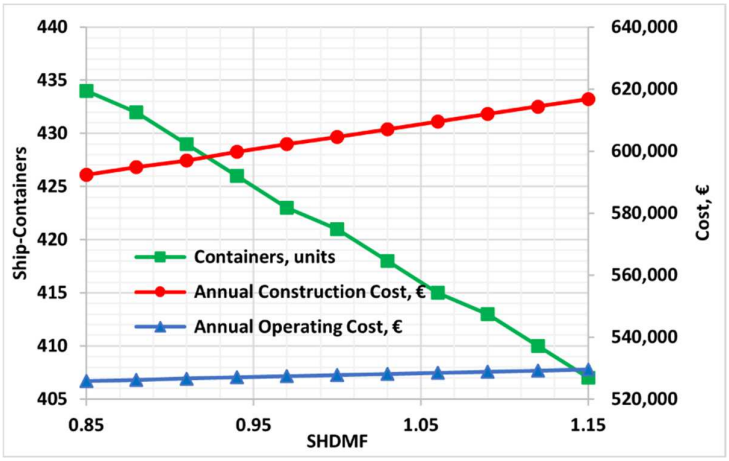

Figure 9. Transported containers, ship annual operating and construction costs.

As seen in Figure 9, the ship construction and operating cost for transporting the same cargo in 20-foot containers are of the same trends, and by increasing *SHDMF*, they are also growing. However, going into a more detailed analysis of different structural design solutions as a function of *SHDMF*, it seems that the number of containers the ship may transport is growing with the reduction in the *SHDMF*.

As shown in Figure 10, for all structural design solutions as a function of *SHDMF*, the relatively more energy-efficient ships indicate a lower level of *EEDI* for the lower *SHDMF*. This can be explained by reducing *SHDMF*, the ship's lightship weight is diminished due to the reduced plate thicknesses. This reduction is compensated by increasing the *DWT* and the respective cargo capacity by keeping the draft constant. The encountered design solution does not involve enhancing the propulsion system and any engineering solution in reducing *EEDI*.

Figure 10. Energy efficiency design index.

MCDM identifies the "best" alternative from pre-selected options, considering a set of several objectives [21–23], which can be a set with multiple equality and inequality type constraints in the decision space [24,25].

The impact of the design parameters on the ship's design solution is analysed using the multi-attribute decision-making Technique of Order Preference by Similarity to Ideal Solution (TOPSIS) [21]. The multi-attribute decision-making aims to identify and choose the best alternatives that fit the design goals. The decision algorithms induce an order on a set of options based on the information [58] about the design descriptions of possible solutions, criteria to measure the performance of solutions, and the preference statements to indicate relative importance.

Eleven ship design alternatives as a function of *SHDMF* are generated and compared. The ideal option, the best level for all attributes considered, and the perfect negative option, which has the worst attribute values, are identified. The TOPSIS method identifies the closest to the ideal solution and farthest from the excellent damaging alternative.

In any ship design solution, $i = 1, \ldots n$ is a function of the design criteria, which are scored, x_{ij} concerning the criterion $j = 1, \ldots m$, where a matrix $\mathbf{X} = (x_{ij})$ of $n \times m$ is developed. C_{11} to C_{2m} are defined based on the ship design, scantling, and strength analysis [21]. $\mathbf{J}^+$ is the set of benefit criteria, where the more significant score represents a better condition. $\mathbf{J}^-$ is the set of negative criteria, where the lower score represents the better condition.

The TOPSIS calculation procedure covers several steps. The first one is the construction of a normalised decision matrix [59]:

$$r_{ij} = \frac{x_{ij}}{\sqrt{\sum x_{ij}^2}} \tag{31}$$

In the next step, the weighted normalised decision matrix is constructed using a set of weights r_{ij} for each criterion w_j:

$$v_{ij} = w_j r_{ij} \tag{32}$$

The positive ideal solution is defined by:

$$A^* = \{v_1^*, \ldots, v_m^*\} \tag{33}$$

where $v_j^* = \{max(v_{ij} \text{ if } j \in \mathbf{J}^+, \ min(v_{ij}) \text{ if } j \in \mathbf{J}^{+\prime})\}$ and the negative ideal solution is defined as:

$$A^* = \{v_1', \ldots, v_m'\} \tag{34}$$

where $v'_j = \{min(v_{ij} \text{ if } j \in \mathbf{J}^-, max(v_{ij}) \text{ if } j \in \mathbf{J}^{-\prime})\}$ and the negative ideal solution is defined as:

The separation measures for each alternative are estimated as [59]:

$$S_i^* = \left[\sum\left(v_j^* - v_{ij}\right)^2\right], \; i = 1, \ldots, n \tag{35}$$

$$S_i' = \left[\sum\left(v_j' - v_{ij}\right)^2\right], \; i = 1, \ldots, n \tag{36}$$

The relative closeness to the ideal solution C_i^* is calculated as:

$$C_i^* = \frac{S_i^*}{S_i^* + S_i'} \; for \; 0 < C_i^* < 1 \tag{37}$$

The option C_i^*, that is closest to 1, is the best-suited solution. In the present study, an inverse multi-attribute decision-making calculation is also performed for any design solution to identify the importance of different criteria, quantified by the maximum relative closeness to the ideal solution. Initially, the weights of all design criteria are assumed to be equal and uniformly distributed. At the end of the calculations, the weights are estimated according to the maximum relative closeness to the ideal design solution and identify the significance of any individual criterion in any specific design solution.

Assuming that the five design criteria have the same weight, 0.2 in the multi-attribute decision-making analysis, the relative closeness to the ideal solution makes the sixth design solution the most acceptable solution at 97.1% significance, followed by the seventh and fifth design solutions (see Figure 11). However, the weight of the design criteria may differ from the assumed uniform distribution here, and a deeper analysis needs to be performed.

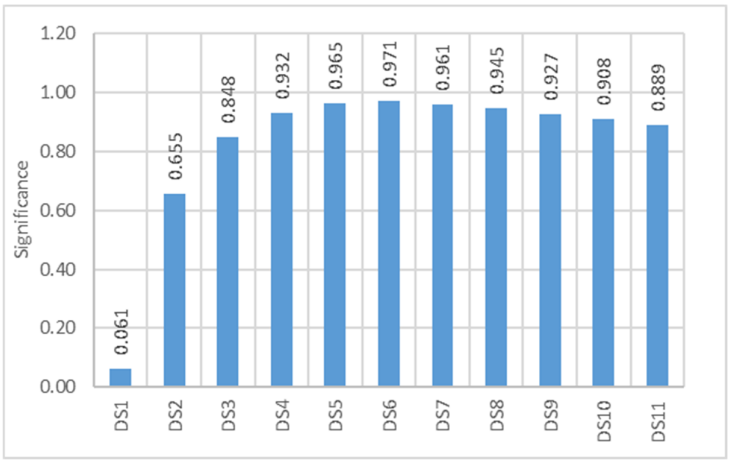

Figure 11. Significance of design solutions.

The inverse calculation is performed to identify the importance of different criteria for the maximum relative closeness to the ideal solution. As can be seen from Figure 12, the best-suited design criterion estimated for the design solution, DS_1. Associated with *SHDMF* = 1 is *EEDI* = 37%, followed by the cargo capacity, represented by the number of containers transported, 22%, the construction cost of 21% and the operating cost of 20%. The risk is not seen as a significant factor for DS_1. However, the DS_1 design solution has the minimum construction and operating cost and maximum cost associated with the risk.

	DS1	DS2	DS3	DS4	DS5	DS6	DS7	DS8	DS9	DS10	DS11
EEDI	0.37	-	0.01	-	-	-	-	-	-	-	-
Containers	0.22	1.00	0.01	0.00	-	-	-	-	-	-	-
Risk	-	-	0.96	0.84	1.00	1.00	1.00	1.00	1.00	1.00	1.00
Construction Cost	0.21	-	0.01	0.01	-	-	-	-	-	-	-
Operating Cost	0.20	-	0.01	0.15	-	-	-	-	-	-	-

Figure 12. Significance of design criterion.

The design solution, $DS_{2,}$ is dominated by the significance of the cargo capacity of 100%. Starting from DS_3, where the significance of the risk dominates, where RISK = 96% and a significance of 4% is estimated for the resting parameters. The significance of the risk is estimated as 84% for DS_4, with an operating cost of 18% and construction cost of 1%. For DS_5 to $DS_{11,}$ the significance of the risk is 100%.

The multi-attribute decision-making approach employed here identifies the best design solution from the alternative design solutions, accounting for the annual operating cost, annual construction cost, risk, cargo capacity, and energy efficiency design index. Design solution 6 is the optimum design solution associated with a beta reliability index of 4.29, annual construction cost of EUR 527,732, operating cost of EUR 604,603, cargo capacity of 412 containers, and energy efficiency design index of 29.24 gCO_2/tonne-mile.

7. Conclusions

The present study developed a design procedure to integrate the innovative risk-based ship hull structural design, capital and operational expenditure, cargo capacity, and energy efficiency for a multi-purpose ship in identifying an optimum level of ship safety, i.e., the optimum reliability index, controlling the risk associated with the ship hull structure. The identified design solution is associated with the minimum expected total cost, leading to lower construction and operational costs, energy efficiency, risk, and maximum cargo capacity. The study used MADM, considering several objectives simultaneously for different scenarios, employing the TOPSIS method, and identifying the best ship structural design solution for all scenarios as a function of SHDMF. It can be noticed that the procedure developed in this work is flexible enough to accommodate different design criteria and possible hazards during the service life of the ship.

The next step of the present study is to adapt the current procedure for the structural design of lightweight ships made of composite materials, including honeycomb sandwich panels replacing the conventional steel structures, to gain benefits of more cargo capacity and cost reduction in building modern energy-efficient and environment-friendly ships.

Author Contributions: T.P. and Y.G. contributed to the probability cost-benefit analysis for ship structural design and implementation, the results analysis, and the manuscript's writing. All authors have read and agreed to the published version of the manuscript.

Funding: This research received no external funding.

Institutional Review Board Statement: Not applicable.

Informed Consent Statement: Not applicable.

Data Availability Statement: The data presented in this study are available within the article.

Acknowledgments: This work was performed within the Strategic Research Plan of the Centre for Marine Technology and Ocean Engineering (CENTEC), which is financed by the Portuguese Foundation for Science and Technology (Fundação para a Ciência e Tecnologia-FCT) under contract UIDB-UIDP/00134/2020.

Conflicts of Interest: The authors declare that they have no conflict of interest.

References

1. Evans, H.J. Basic Design Concepts. *J. Am. Soc. Nav. Eng.* **1959**, *71*, 671–678. [CrossRef]
2. Nowacki, H.; Brusis, F.; Swift, P. Tanker preliminary design—An optimisation problem with constraints. *Trans. Soc. Nav. Archit. Mar. Eng.* **1970**, *78*, 357–390.
3. Hughes, O. *Ship Structural Design, A Rational-Based, Computer-Aided, Optimization Approach*; Joh Wiley & Sons: Hoboken, NJ, USA, 1983.
4. Hughes, O.F.; Mistree, F.; Zanic, V. A practical method for the rational design of ship structures. *J. Ship Res.* **1980**, *24*, 101–113. [CrossRef]
5. Seo, S.I.; Son, K.H.; Park, M.K. Optimum structural design of naval vessels. *Mar. Technol. Soc. Nav. Archit. Mar. Eng.* **2003**, *40*, 149–157.
6. Khajehpour, S.; Grierson, D.E. Profitability versus safety of high-rise office buildings. *Struct. Multidiscip. Optim.* **2003**, *25*, 279–293. [CrossRef]
7. Parsons, M.G.; Scott, R.L. Formulation of multi-criterion design optimisation problems for solution with scalar numerical optimisation methods. *J. Ship Res.* **2004**, *48*, 61–76. [CrossRef]
8. Klanac, A.; Kujala, P. Optimal design of steel sandwich panel applications in ships. In Proceedings of the 9th Symposium on Practical Design of Ships and Other Floating Structures (PRADS), Lubeck-Travemuende, Germany, 12–17 September 2004; pp. 907–914.
9. Cho, K.; Arai, M.; Basu, R.; Besse, P.; Birmingham, R.; Bohlmann, B.; Boonstra, H.; Chen, Y.; Hampshire, J.; Hung, C.; et al. Design Principles and Criteria. In Proceedings of the 15th International Ship and Offshore Structures Congress (ISSC), Southampton, UK, 20–25 August 2006; pp. 521–599.
10. Zanic, V.; Andric, J.; Prebeg, P. Superstructure deck effectiveness of the generic ship types—A concept design methodology. In Proceedings of the 11th International Congress of International Maritime Association of the Mediterranean (IMAM), Lisbon, Portugal, 26–30 September 2005; pp. 579–588.
11. Xuebin, L. Multiobjective optimisation and multiattribute decision making study of ship's principal parameters in conceptual design. *J. Ship Res.* **2009**, *53*, 83–92. [CrossRef]
12. IMO. Revised Guidelines for Formal Safety Assessment (FSA) for Use in the IMO Rule-Making Process. Available online: https://www.liscr.com/revised-guidelines-formal-safety-assessment-fsa-use-imo-rule-making-process (accessed on 18 June 2022).
13. IMO. *Formal Safety Assessment on Crude Oil Tankers*; International Maritime Organization Publishing: Fort Lauderdale, FL, USA, 2008.
14. IMO. Amendments to the Guidelines for Formal Safety Assessment (FSA) for Use in the IMO Rule-Making Process. Available online: http://docs.yasinskiy.net/books/imo-msc-circ/1180.pdf (accessed on 18 June 2022).
15. IMO. Consolidated Text of the Guidelines for Formal Safety Assessment (FSA) for Use in the IMO Rule-Making Process. Available online: https://wwwcdn.imo.org/localresources/en/OurWork/HumanElement/Documents/1023-MEPC392.pdf (accessed on 18 June 2022).
16. Papanikolaou, A.D.; Guedes Soares, C.; Jasionowski, A.; Jensen, J.J.; McGeorge, D.; Poylio, E.; Vassalos, D. *Risk-Based Ship Design*; Springer: Berlin/Heidelberg, Germany, 2009.
17. Papadimitriou, S.; Koliousis, I.G.; Sdoukopoulos, E.; Lyridis, D.V.; Tsioumas, V.; Stavroulakis, P.J. *The Dynamics of Short Sea Shipping. New Practices and Trends*; Palgrave Macmillan: Cham, Switzerland, 2018.
18. Garbatov, Y.; Ventura, M.; Guedes Soares, C.; Georgiev, P.; Koch, T.; Atanasova, I. Framework for conceptual ship design accounting for risk-based life cycle assessment. In *Maritime Transportation and Harvesting of Sea Resources*; Guedes Soares, C., Teixeira, A., Eds.; Taylor & Francis Group: London, UK, 2018; pp. 921–931.
19. Garbatov, Y.; Sisci, F.; Ventura, M. Risk-based framework for ship and structural design accounting for maintenance planning. *Ocean Eng.* **2018**, *166*, 12–25. [CrossRef]
20. Garbatov, Y. Risk-based corrosion allowance of oil tankers. *Ocean Eng.* **2020**, *213*, 107753. [CrossRef]
21. Hwang, C.L.; Yoon, K. Multiple attribute decision making, methods and applications. In *Lecture Notes in Economics and Mathematical Systems*; Springer-Verlag: New York, NY, USA, 1981; Volume 186.
22. Tzeng, G.-H.; Huang, J.-J. *Multiple Attribute Decision Making (Methods and applications)*; CRC Press—Taylor & Francis Group: New York, NY, USA, 2011.
23. Mardani, A.; Jusoh, A.; Nor, K.; Khalifah, Z.; Zakwan, N.; Valipour, A. Multiple criteria decision-making techniques and their applications—A review of the literature from 2000 to 2014. *Econ. Res. -Ekon. Istraživanja* **2015**, *28*, 516–571. [CrossRef]
24. Kaliszewski, I. *Soft Computation for Complex Multiple Criteria Decision Making*; Springer: New York, NY, USA, 2006.
25. Miettinen, K.; Hakanen, J.; Podkopaev, D. Interactive Nonlinear Multiobjective Optimization Methods. In *Multiple Criteria Decision Analysis: State of the Art Surveys*; Greco, S., Ehrgott, M., Figueira, J.R., Eds.; Springer Science+Business Media: Berlin/Heidelberg, Germany, 2016; Volume 233, pp. 931–980.

26. Garbatov, Y.; Almany, N.; Tekgoz, M. Operational Behaviour of an Offshore Multi-purpose Support Vessel in the Eastern Mediterranean Sea. *Int. J. Marit. Eng.* **2019**, *161*, A303–A312. [CrossRef]
27. Garbatov, Y.; Huang, Y.C. Multiobjective Reliability-Based Design of Ship Structures Subjected to Fatigue Damage and Compressive Collapse. *J. Offshore Mech. Arct. Eng.* **2020**, *142*, 051701. [CrossRef]
28. Horn, J.; Nafpliotis, N.; Goldberg, D. A niched Pareto genetic algorithm for multiobjective optimisation. In Proceedings of the IEEE World Congress on Computational Intelligence, Orlando, FL, USA, 27–29 June 1994; pp. 82–87.
29. Garbatov, Y.; Georgiev, P. Advances in conceptual ship design accounting for the risk of environmental pollution. *Annu. J. Tech. Univ. Varna* **2021**, *5*, 25–41. [CrossRef]
30. *NR467*; Rules for the Classification of Steel Ships. Bureau Veritas: Neuilly-sur-Seine, France, 2019.
31. Garbatov, Y.; Georgiev, P. Risk-based conceptual ship design of a bulk carrier accounting for energy efficiency design index (EEDI). *Int. J. Marit. Eng.* **2021**, *163*, A51–A62. [CrossRef]
32. Garbatov, Y.; Parunov, J.; Kodvanj, J.; Saad-Eldeen, S.; Guedes Soares, C. Experimental assessment of tensile strength of corroded steel specimens subjected to sandblast and sandpaper cleaning. *Mar. Struct.* **2016**, *49*, 18–30. [CrossRef]
33. Garbatov, Y.; Tekgoz, M.; Guedes Soares, C. Experimental and numerical strength assessment of stiffened plates subjected to severe non-uniform corrosion degradation and compressive load. *Ships Offshore Struc* **2016**, *12*, 461–473. [CrossRef]
34. Woloszyk, K.; Garbatov, Y.; Kowalski, J. Indoor accelerated controlled marine corrosion testing of small- and large-scale specimens. *Ocean Eng.* **2021**, *241*, 110039. [CrossRef]
35. Zima, B.; Woloszyk, K.; Garbatov, Y. Corrosion degradation monitoring of ship stiffened plates using guided wave phase velocity and constrained convex optimisation method. *Ocean Eng.* **2022**, *253*, 111318. [CrossRef]
36. Woloszyk, K.; Garbatov, Y.; Klosowski, P. Stress-strain model of lower corroded steel plates of normal strength for fitness-for-purpose analyses. *Constr. Build. Mater.* **2022**, *323*, 126560. [CrossRef]
37. *MARS2000*; Rules for the Classification of Ships and IACS Common Structural Rules for Bulk Carriers and Tankers. Bureau Veritas: Neuilly-sur-Seine, France, 2011.
38. Smith, C. Influence of Local Compressive Failure on Ultimate Longitudinal Strength of a Ship Hull. In Proceedings of the International Symposium on Practical Design in Shipbuilding (PRADS), Tokyo, Japan, 18–20 October 1977; pp. 73–79.
39. Horte, T.; Wang, W.; White, N. Calibration of the hull girder ultimate capacity criterion for double hull tankers. In Proceedings of the 10th International Symposium on Practical Design of Ships and Other Floating Structures (PRADS), Houston, TX, USA, 1 January 2007; pp. 235–246.
40. Guia, J.; Teixeira, A.P.; Guedes Soares, C. Sensitivity analysis on the optimum hull girder safety level of a Suezmax tanker. In *Marine Technology and Engineering*; Guedes Soares, C., Santos, T.A., Eds.; Taylor & Francis Group: London, UK, 2016; Volume 3, pp. 823–830.
41. Guedes Soares, C.; Dogliani, M.; Ostergaard, C.; Parmentier, G.; Pedersen, P.T. Reliability Based Ship Structural Design. *Trans. Soc. Nav. Archit. Mar. Eng.* **1996**, *104*, 359–389.
42. Guedes Soares, C.; Moan, T. Statistical Analysis of Still—Water Bending Moments and Shear Forces on Tankers and Bulk Carriers. *Nor. Marit. Res.* **1982**, *10*, 33–47.
43. Guedes Soares, C.; Moan, T. Statistical Analysis of Still-Water Load. Effects in Ship Structures. *SNAME Trans.* **1988**, *96*, 129–156.
44. Guedes Soares, C. Stochastic Modelling of Maximum Still-Water Load Effects in Ship Structures. *J. Ship Res.* **1990**, *34*, 199–205. [CrossRef]
45. Garbatov, Y.; Guedes Soares, C. Reliability assessment of a container ship subjected to asymmetrical bending. In Proceedings of the 13th International Symposium on Practical design of ships and other floating structures (PRADS2016), Copenhagen, Denmark, 4–8 September 2016; p. D155.
46. Garbatov, Y.; Guedes Soares, C.; Wang, G. Nonlinear Time-Dependent Corrosion Wastage of Deck Plates of Ballast and Cargo Tanks of Tankers. *J. Offshore Mech. Arct. Eng.* **2007**, *129*, 48–55. [CrossRef]
47. Rackwitz, R.; Filessler, B. Structural Reliability under Combined Random Load Sequences. *Comput. Struct.* **1978**, *9*, 489–494. [CrossRef]
48. Gollwitzer, S.; Rackwitz, R. First-Order System Reliability of Structural System. In Proceedings of the 4th International Conference on Structural Safety and Reliability, Kobe, Japan, 27–29 May 1985; pp. 171–218.
49. Cornell, C. A Probability-Based Structural Code. *J. Am. Concr. Inst. J.* **1969**, *66*, 974–985.
50. MARAD. United States Maritime Administration (MARAD). Guideline Specifications for Merchant Ship Construction. Available online: https://maritime.dot.gov/ports/national-maritime-resource-and-education-center/marad-guideline-specifications-merchant-ship (accessed on 18 June 2022).
51. Garbatov, Y.; Ventura, M.; Georgiev, P.; Damyanliev, T.P.; Atanasova, I. Investment cost estimate accounting for shipbuilding constraints. In *Maritime Transportation and Harvesting of Sea Resources*; Guedes Soares, C., Teixeira, A., Eds.; Taylor & Francis Group: London, UK, 2018; pp. 913–921.
52. Steelbenchmarker. Dollars Per-Metric Tonne-Steel. Available online: http://www.steelbenchmarker.com/specifications (accessed on 18 June 2022).
53. Skjong, R.; Vanem, E.; Endersen, Ø. Risk Evaluation Criteria, SAFEDOR. Available online: www.safedor.org/resources/index.html (accessed on 18 June 2022).
54. OCDE. *OCDE Factbook-Economic, Environmental and Social Statistics*; OCDE: Paris, France, 2014; pp. 96–106.

55. Moan, T.; Shu, Z.; Drummen, I.; Amlashi, H. Comparative reliability analysis of ships—Considering different ship types and the effect of ship operations on loads. *Trans. Soc. Nav. Archit. Mar. Eng.* **2007**, *114*, 16–54.
56. Benford, H. *The Practical Application of Economics of Merchant Ship Design*; The Society of Naval Architecture and Marine Engineering: New Jersey, NJ, USA, 1967.
57. Cudina, P.; Zanic, V.; Preberg, P. Multiattribute Decision Making Methodology in the Concept Design of Tankers and Bulk-Carriers. In Proceedings of the 11th Symposium on Practical Design of Ships and Other Floating Structures, PRADS, Rio de Janeiro, Brazil, 19–24 September 2010.
58. Aspen, D.M.; Sparrevik, M.; Fet, A.M. Review of methods for sustainability appraisals in ship acquisition. *Environ. Syst. Decis.* **2015**, *35*, 323–333. [CrossRef]
59. Moore, L.J.; Taylor, B.W.; Clayton, E.R.; Lee, S.M. Analysis of a multi-criteria project crashing model. *AIIE Trans.* **1978**, *10*, 163–210. [CrossRef]